

# Performance characteristics of $\text{In}_{0.53}\text{Ga}_{0.47}\text{As}/\text{In}_{0.52}\text{Al}_{0.48}\text{As}$ modulation-doped field-effect transistors realized by two-step epitaxy: Effects of molecular-beam epitaxial regrowth

R. Lai and P. K. Bhattacharya

Center of High-Frequency Microelectronics and Department of Electrical Engineering and Computer Science, The University of Michigan, Ann Arbor, Michigan 48109-2122

(Received 1 November 1989; accepted for publication 9 January 1990)

Epitaxial regrowth is emerging as an important step in the processing and realization of optoelectronic integrated circuits. We have studied the dc and microwave characteristics of regrown  $\text{In}_{0.53}\text{Ga}_{0.47}\text{As}/\text{In}_{0.52}\text{Al}_{0.48}\text{As}$  modulation-doped field-effect transistors on InP substrates and have compared these with the characteristics of normally grown devices. The low-field transport properties of the heterostructures are degraded due to the increased interface roughness caused by processing and regrowth. The dc and microwave characteristics in terms of  $g_m$  (300 mS/mm),  $f_T$  (20 GHz), and  $f_{\max}$  (35 GHz) are slightly degraded in the regrown devices compared to the normally grown ones. The density of states at the active heterointerface is not appreciably increased compared to normally grown devices. The low-frequency  $1/f$  noise level is higher in the saturation regime in the regrown devices. Our results indicate that there may be increased density of trapping centers in the regrown  $\text{In}_{0.52}\text{Al}_{0.48}\text{As}$  buffer layer below the active channel.

## I. INTRODUCTION

A major problem often encountered in the design of optoelectronic integrated circuits (OEICs) is the incompatibility in layer structure between the electrical device and the optical device. This incompatibility has been previously circumvented either by the use of vertical integrated structures or by regrowth techniques. Vertical integration structures involve the stacking of electrical and optical devices on top of each other.<sup>1</sup> This strategy can suffer from inferior performance due to capacitive effects. An alternative approach is planar integration which involves the regrowth of the electrical device next to the optical device. We have recently studied<sup>2</sup> the interface region generated by molecular-beam epitaxial regrowth of GaAs in detail. Regrowth was carried out on epitaxial GaAs after a variety of realistic device processing steps. Combinations of wet chemical etching and ion milling with and without annealing were used with the objective of establishing the best procedure for integrated technologies during regrowth. Our data favor the concept of a disordered region created at the interface during regrowth. We have measured interface state and trap densities and it was seen that the values of these parameters are very much dependent on the type of processing before regrowth. To our knowledge, no such data exist for the regrowth of InP-based compounds. In particular, it is important to establish the effects of conventional regrowth on the performance of electronic and optical devices placed close to the regrowth interface.

The ternary  $\text{In}_{0.53}\text{Ga}_{0.47}\text{As}/\text{In}_{0.52}\text{Al}_{0.48}\text{As}$  heterostructure latticed matched to InP can be used in the 1.3–1.55  $\mu\text{m}$  wavelength region where minimum dispersion and attenuation are seen in optical fibers, and is therefore an excellent candidate for application in optical communication systems. Furthermore, this heterostructure also exhib-

its excellent electrical properties. For example, in InGaAs/InAlAs modulation-doped field-effect transistors (MODFETs), the high mobility of the InGaAs coupled with the large conduction-band discontinuity between InGaAs and InAlAs results in state-of-the-art performance for these devices.<sup>3</sup> We report here the characteristics of InGaAs/InAlAs MODFETs fabricated adjacent to ridge waveguides by molecular-beam epitaxial (MBE) regrowth and subsequent lithography. The waveguide structures were designed for electro-optic phase modulators which are not the subject of this paper. It should be noted, however, that this scheme of regrowth is also applicable to a laser integrated monolithically with a FET driver. In particular, we have compared the properties of regrown MODFETs with identical normally grown devices.

## II. EXPERIMENTAL TECHNIQUES

The waveguide phase shifter structure was first grown on a semi-insulating InP substrate in a Varian GEN II system followed by the MODFET structure, and both are schematically shown in Fig. 1.  $\text{SiO}_2$  was then deposited on the layer using plasma-enhanced chemical vapor deposition (PECVD) and holes were subsequently etched for regrowth of the MODFET heterostructure. A calibration InP substrate was also loaded next to the regrowth sample. The MODFET structure was designed such that the pinch-off voltage would be about  $-1.0$  V and the critical voltage, defined to be the voltage at which parallel conduction begins to occur, was around 0 V. A GaAs cap layer was used to help eliminate the need for gate recess during the processing of the device.<sup>4</sup> After the regrowth of the MODFET, the  $\text{SiO}_2$  layer and the polycrystalline material above it were selectively etched off, leaving the MODFET and waveguide structures adjacent to each other. A surface in-

| waveguide               |  | MODFET                  |  |
|-------------------------|--|-------------------------|--|
| p+ InAlAs               | $4 \times 10^{18} \text{ cm}^{-3}$ 0.1 $\mu\text{m}$ | n GaAs                  | $5 \times 10^{17} \text{ cm}^{-3}$ 10 nm |
|                         |  | n+ InAlAs               | $3 \times 10^{18} \text{ cm}^{-3}$ 20 nm |
|                         |  | undoped InAlAs          | 5 nm                                     |
|                         |  | undoped InGaAs          | 60 nm                                    |
| undoped InGaAs          | 1.2 $\mu\text{m}$                                    | undoped InAlAs          | 0.5 $\mu\text{m}$                        |
|                         |  | InGaAs/InAlAs SL buffer | 0.36 $\mu\text{m}$                       |
| n+ InAlAs               | $3 \times 10^{18} \text{ cm}^{-3}$ 0.6 $\mu\text{m}$ | undoped InAlAs          | 0.5 $\mu\text{m}$                        |
| InGaAs/InAlAs SL buffer | 0.12 $\mu\text{m}$                                   | InGaAs/InAlAs SL buffer | 0.36 $\mu\text{m}$                       |

Semi-Insulating InP Substrate

FIG. 1. Schematic of the MBE regrown MODFET structure next to the waveguide phase shifter.

spection under the microscope showed that the regrowth sample was slightly rougher than the normally grown one.

Hall measurements were done on both the normal and regrown MODFET structures. For the normally grown MODFET, the mobilities are 11 100 and 41 000  $\text{cm}^2 \text{V}^{-1} \text{s}^{-1}$  at 300 and 77 K, respectively, and the sheet carrier densities are  $2.2 \times 10^{12}$  and  $2.1 \times 10^{12}/\text{cm}^2$  at 300 and 77 K, respectively. In comparison, the regrown sample yielded mobilities of 7100 and 14 400  $\text{cm}^2 \text{V}^{-1} \text{s}^{-1}$  at 300 and 77 K, respectively, with sheet carrier densities of  $2.4 \times 10^{12}$  and  $2.1 \times 10^{12}/\text{cm}^2$  at 300 and 77 K, respectively. We attribute the large decrease in the mobility in the regrown sample to an increase in interface roughness scattering.<sup>5</sup>

Transistors were made with the normally grown and regrown heterostructures using standard photolithography and liftoff techniques.<sup>4</sup> The gate was formed by evaporating 500 Å Ti/3000 Å Au. A scanning electron microscope (SEM) inspection of the gate stripes showed that the gate lengths varied from 0.9 to 1.1  $\mu\text{m}$  on both samples. Finally, a thick 1000 Å Ti/10 000 Å Au metallization was evaporated and lifted off to form the interconnect level used for the microwave testing.

### III. DEVICE CHARACTERISTICS: DISCUSSION OF RESULTS

Typical dc characteristics are shown in Figs. 2(a) and 2(b) for the normally grown and regrown devices, respectively. In general, the normally grown devices showed larger transconductance and larger drain current values. Also, the output conductance was found to be higher in the regrown devices compared to the normally grown ones. The kink effect, where a negative resistance can be seen

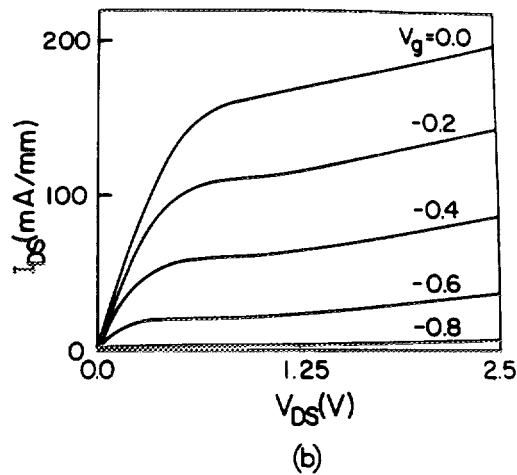
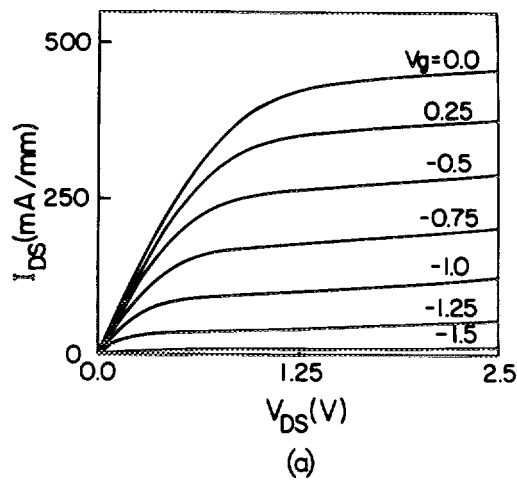
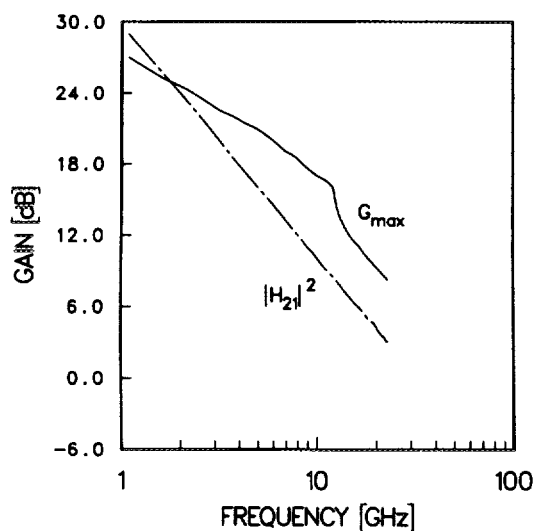


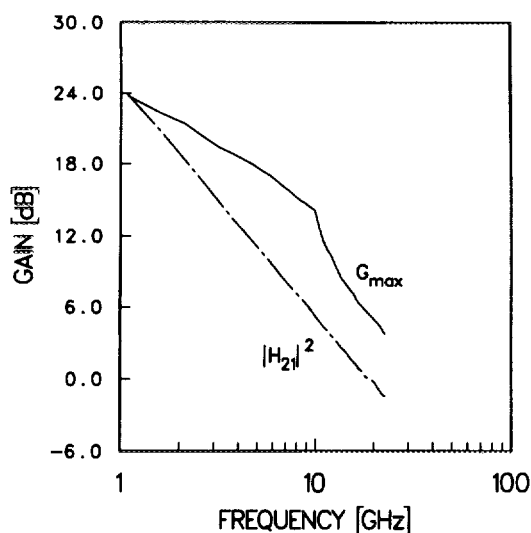
FIG. 2. Drain current-voltage characteristics of (a) normally grown and (b) regrown MODFET devices with a  $1.0 \times 100 \mu\text{m}^2$  gate.

slightly past the knee voltage of the  $I_{ds}$  vs  $V_{ds}$  characteristic, seemed to be more evident in the regrown devices than in the normally grown devices. It is generally believed that the kink in the transistor characteristics is due to trapping and detrapping in the buffer layer beneath the active channel. It has been shown recently<sup>3</sup> that by growing the InAlAs buffer at very low temperatures, in which the trapping/recombination times are made very short, the kink effect is greatly reduced. We believe that the density of slow traps is increased in the regrown InAlAs underneath the channel.

Typical microwave characteristics for the normally grown and regrown samples are shown in Figs. 3(a) and 3(b). The normally grown devices showed a cutoff frequency  $f_T$  ranging from 25 to 32 GHz and a maximum oscillating frequency  $f_{max}$  ranging from 45 to 55 GHz while the regrown devices showed  $f_T$  ranging from 13 to 20 GHz and  $f_{max}$  ranging from 25 to 35 GHz. From the dc measured data and the equivalent circuit obtained by fitting the measured S parameters, it is evident that the main



(a)

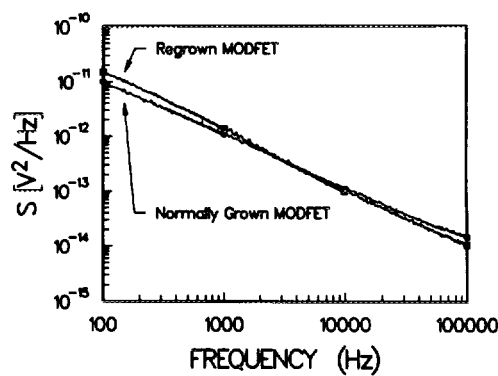


(b)

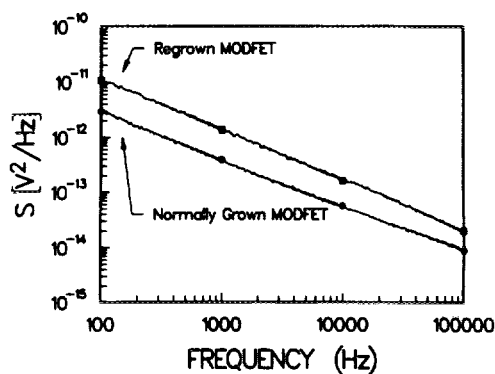
FIG. 3. Variation of current gain and maximum available gain with frequency for (a) normally grown and (b) regrown MODFET devices with a  $1.0 \times 100 \mu\text{m}^2$  gate.

contributors to inferior microwave performance in the regrown devices are a larger source resistance, a larger output conductance, and a lower  $g_m$  value.

Figure 4(a) shows the average input low-frequency noise spectrum measured for typical regrown and normally grown devices operating in the linear region of the MODFET. All the measurements showed approximately a  $1/f$  characteristic. As can be seen from the figure, the regrown and normally grown devices showed very little difference in noise level. Typical noise levels at 10 kHz were around  $10^{-13} \text{ V}^2/\text{Hz}$ . When the devices are operated in the saturation region, however, the noise level of the normally grown devices dropped lower than the regrown devices as shown in Fig. 4(b). Typical noise levels at 10 kHz were between 1 and  $5 \times 10^{-13} \text{ V}^2/\text{Hz}$  for the regrown devices



(a)



(b)

FIG. 4. Average input low-frequency noise spectrum of normally grown and regrown MODFET devices operating (a) in the linear region ( $V_{ds} = 0.2 \text{ V}$ ) and (b) in the saturation region ( $V_{ds} = 1.5 \text{ V}$ ).

and between  $5 \times 10^{-14}$  and  $1 \times 10^{-13} \text{ V}^2/\text{Hz}$  for the normally grown devices. The approximately  $1/f$  noise characteristic for both the regrowth and the normal devices indicates that generation-recombination due to interface state traps may not be a dominant mechanism of the low-frequency noise at the measured frequencies, although the noise characteristics were not measured at lower temperatures.<sup>6</sup> As observed by Ng *et al.*,<sup>7</sup> the noise level decreased from the linear region to the saturation region for the normally grown device.

To investigate the interface state characteristics, ac conductance measurements were made on the regrowth samples. The technique has been discussed in detail in an earlier publication.<sup>8</sup> The measured variations of the interface state density,  $D_{it}$ , and emission time constant,  $\tau$ , on gate bias are shown in Fig. 5. The typical  $D_{it}$  values were in the  $10^{12} \text{ eV}^{-1} \text{ cm}^{-2}$  range while  $\tau$  was generally between 5 and 50 ns. These values are not significantly different from the values obtained with InGaAs/InAlAs lattice-matched MODFETs,<sup>7,8</sup> and signify that the regrown devices do not have a higher density of interface states near the channel compared to the normally grown ones.

Because of a nonideal substrate preparation before the regrowth step, a degradation in the performance of the regrown MODFET is expected. This would result from

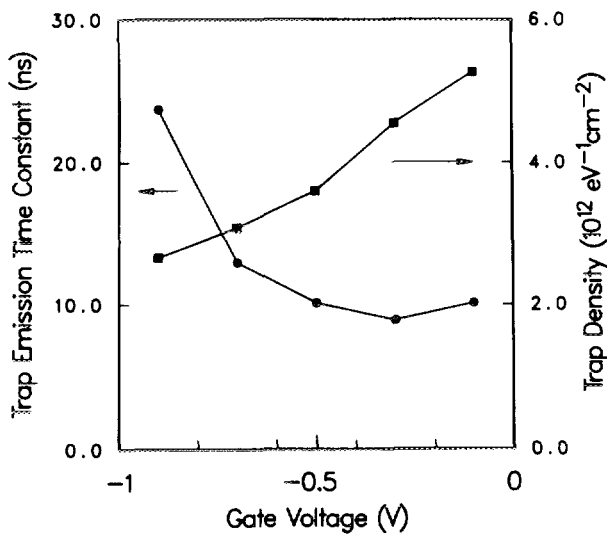


FIG. 5. Variation of the interface state density,  $D_{it}$ , and interface trap emission time constant,  $\tau$ , with applied gate to source voltage,  $V_{gs}$ , in regrown MODFET.

(a) increased interface roughness, (b) increased nonradiative interface states density which may be related to the interface roughness, or (c) impurities and related defects outdiffusing or riding on the growing surface. We attribute the degradation of the channel transport properties in the regrown MODFET to increased interface roughness, compared to the normally grown structure. The measured density of interface states, on the other hand, is not larger than in a normally grown MODFET. We believe, therefore, that the higher  $1/f$  noise level in the regrown device and the enhanced kink effect result from impurities or defects outdiffusing from the regrown interface and riding with the growth surface.

#### IV. CONCLUSIONS

We have shown the results of the dc and microwave characteristics of regrown  $\text{In}_{0.53}\text{Ga}_{0.47}\text{As}/\text{In}_{0.52}\text{Al}_{0.48}\text{As}$  MODFETs on InP substrates. These devices showed slight degradation in  $g_m$ ,  $f_T$ , and  $f_{max}$  compared to normally

grown MODFETs. The measured density of interface states at the active heterointerface of the regrown devices is not appreciably increased compared to normally grown MODFETs. However, the low-frequency  $1/f$  noise level is higher in the regrown devices than the normally grown devices in the saturation regime. We believe that the inferior low-field transport properties of the regrown heterostructure are due to increased interface roughness at the heterointerface, and degrade the overall device dc and microwave performance. Furthermore, the observed increase in low-frequency  $1/f$  noise level and occurrence of the kink effect indicate an increase in the density of trapping centers in the regrown  $\text{In}_{0.52}\text{Al}_{0.48}\text{As}$  buffer layer below the active channel. Further work should focus on regrowth techniques to help smoothen out the growth front and to reduce the number of defects and impurities outdiffusing from the regrown interface.

#### ACKNOWLEDGMENTS

The authors would like to acknowledge G. I. Ng for help in low-frequency and interface state density measurements, M. Tutt for help in microwave measurements, D. Pavlidis for helpful discussions, and J. Pamulapati for MBE growth and regrowth of the structures. The work was supported by the Army Research Office (URI Program) under Contract No. DAAL03-87-K-0007.

- <sup>1</sup>S. Miura, O. Wada, H. Hamguchi, M. Ito, M. Makiuchi, K. Nakai, and T. Sakurai, *IEEE Electron Device Lett.* **4**, 375 (1983).
- <sup>2</sup>D. Biswas, P. R. Berger, U. Das, J. E. Oh, and P. K. Bhattacharya, *J. Electron. Mater.* **18**, 137 (1981).
- <sup>3</sup>U. K. Mishra, A. S. Brown, and J. F. Jensen, presented at the 16th International Symposium on Gallium Arsenide and Related Compounds, Kamizawa, Japan, 1989 (to appear in *Inst. Phys. Conf. Series*, edited by T. Ikawa, Bristol, 1990).
- <sup>4</sup>W. P. Hong and P. K. Bhattacharya, *IEEE Electron Device Lett.* **9**, 352 (1988).
- <sup>5</sup>W. P. Hong, J. Singh, and P. K., Bhattacharya, *IEEE Electron Device Lett.* **7**, 480 (1986).
- <sup>6</sup>S. Kugler, *IEEE Trans. Electron Devices* **35**, 623 (1988).
- <sup>7</sup>G. I. Ng, A. Reynoso, J. E. Oh, D. Pavlidis, J. Graffeuil, P. K. Bhattacharya, M. Weiss, and K. Moore, presented at the Cornell Conference, Ithaca, NY, 1989.
- <sup>8</sup>W. P. Hong, J. E. Oh, P. K. Bhattacharya, and T. E. Tiwald, *IEEE Trans. Electron Devices* **35**, 1585 (1988).